Hidden species diversity in *Pachyhynobius*: a multiple approaches species delimitation with mitogenomes

Tao Pan[a,b†], Zhonglou Sun[a,c†], Xinlei Lai[a], Pablo Orozco-terWengel[d], Peng Yan[b], Guiyou Wu[a], Hui Wang[a], Weiquan Zhu[c], Xiaobing Wu [b]*, Baowei Zhang[a]*

[a] Anhui Key Laboratory of Eco-engineering and Bio-technique, School of Life Sciences, Anhui University, Hefei 230601, Anhui, China

[b] School of Life Sciences, Anhui Normal University, Wuhu 241000, Anhui, China

[c] Department of Medicine, University of Utah, Salt Lake City 84112, Utah, United States

[d] School of Biosciences, Cardiff University, Cardiff, United Kingdom

† These authors contributed equally to this work.

*Corresponding author

E-mail address: zhangbw@ahu.edu.cn (Baowei Zhang), wuxb@ahnu.edu.cn (Xiaobing Wu).

Running title: Species delimitation of *Pachyhynobius*

ABSTRACT

The lack of distinct morphological features of cryptic species is a hard problem for taxonomy, especially when the taxa are closely related with considerable amounts of ancestral polymorphism. Lately, intensive coalescent-based analyses involving multiple loci have become the preferred method to assess the extent of genetic distinctivness in otherwise phenotypically similar populations. Previously, phylogenetic studies on *Pachyhynobius shangchengensis* uncovered five extremely deeply divergent clades, which suggested that this species may be a cryptic species complex. In this study, we used the complete mitochondrial genome data and samples from the entire range of stout salamander (*Pachyhynobius*), as well as publicly available mitochondrial genomes to assess species boundaries within this genus using a suite of diverse methodologies (e.g. general mixed Yule coalescent model, Automatic Barcode Gap Discovery). The phylogenetic relationships recovered two major groups within *P. shangchengensis*, with one group formed by four of the six extant populations and corresponding to the central and eastern range of the Dabie mountains, while the other group encompassed two other lineages in the north west of the Dabie mountain range. The species delimitation comparison within *Pachyhynobius* supported the presence of recognized species within the genus, and consensus was observed across methods for the existence of up to five cryptic species within what has been traditionally considered to be *P. shangchengensis*. While this implies the existence of four taxa in addition to the described *P. shangchengensis* species, morphological data and life history information are further required to

contribute to the species definition. The observed pattern of genetic variation is likely the outcome of a discontinuous habitat combined with niche conservatism, which produced the sky-island effect observed in *Pachyhynobius*, and which led to formation of a hidden species diversity in this genus.

Keywords: Dabie Mountains; Species delimitation; *Pachyhynobius*; mitochondrial genome; cryptic species.

1. Introduction

There is ongoing debate regarding numerous species concepts that emphasize different criteria for delimiting species (Aldhebiani, 2018; Hausdorf, 2011). Regardless of definition, accurate and objective species delimitation is extremely important as species are considered the fundamental unit in many fields such as biogeography, macroevolution, ecology and conservation biology (Agapow et al., 2004; Sites and Marshall, 2003, 2004). Traditionally, species have been identified and described using qualitative or quantitative morphological features (Aldhebiani, 2018; Hausdorf, 2011). For some organisms, the description of independent evolutionary lineages appears to be straightforward due to the existence of diagnostic morphological features that represent different selection trajectories or differences that may have resulted from genetic drift after long-term isolation (Lande, 1976). However, for many organisms, especially those with non-visual mating approaches (Bickford et al., 2007), if the diagnostic morphological features are subtle or even

non-existent, species identification based solely on morphological differences may be problematic (Kajtoch et al., 2017; Kotsakiozi et al., 2018; Shirley et al., 2014). In addition, for some organisms, similar selection pressures or extreme environments may result in morphological features experiencing convergent evolution (Nevo, 2001). Morphological variation may be the result of phenotypic plasticity or short-term adaptation to local conditions (Dowle et al., 2015; Svanback and Eklov, 2006; Wagner et al., 2013), a process that further makes species delimitation by morphological differences challenging. Therefore, morphology-based taxonomy may relatively underestimate species number due to the presence of cryptic species, which provide opportunities and challenges for species delimitation based on phylogenetic data (Catarina et al., 2016; Giarla et al., 2014; Kotsakiozi et al., 2018; Sheridan and Stuart, 2018).

With the development of species genetic delimitation, various methods have recently been proposed to assess the putative hidden species with evolutionary independence using phylogenetic data. The Bayes factor (BF) approach (Grummer et al., 2013) is based on the marginal-likelihood estimates (MLE) via path-sampling (PS) or stepping-stone sampling (SS) analyses to identify the most suitable species delimitation model across multiple simulated hypotheses (Fan et al., 2011; Li and Drummond, 2012; Xie et al., 2011). Similarly, the Bayesian Phylogenetics and Phylogeography (BPP) is a species-delimitation approach that simultaneously takes into account the phylogenetic uncertainty and stochastic lineage sorting in a dataset to estimate the posterior probability of species assignment, however, conditioning the

86 species assignment to a single user-defined species tree (Yang and Rannala, 2010).
87 BPP estimates the distribution of genealogies for each locus and by testing multiple
88 permutations of the species tree it enables identifying the optimal species delimitation.
89 Coalescent-based methods like the general mixed Yule coalescent model (GMYC)
90 have become an important tree-based species-delimitation approach, although they are
91 often applied to barcoding data, which may not be the most suitable loci for
92 phylogenetic reconstruction (e.g. mitochondrial DNA genes) (Fujisawa and
93 Barraclough, 2013; Fujita and Al, 2012; Leaché and Fujita, 2010; Pons et al., 2006).
94 In GMYC models a maximum likelihood and an ultrametric gene tree is used to
95 simulate the transition threshold between inter- and intra-specific branching patterns,
96 with branching events older than the inferred threshold indicating speciation event,
97 while younger ones represent coalescences within species. For GMYC the putative
98 species number equals the number of lineages crossing the threshold. Similar to
99 GMYC, the Poisson tree processes (PTP/bPTP) model is used to estimate the
100 transition in branch lengths between versus within species (Zhang et al., 2013). PTP
101 calculates the branching process by estimating the expected number of substitutions
102 based on a nonparametric phylogenetic tree. Lastly, Automatic Barcode Gap
103 Discovery (ABGD) employs a different approach, which distinguishes the partitions
104 of the genetic distances among a group of individuals based on clustering algorithms
105 and then infers a final array of putative species (Puillandre et al., 2012a). These
106 species-delimitation methods have been successfully used to identify boundaries for
107 species complexes of morphologically undistinguishable species suggesting that they

are fairly robust to model assumptions (Blair and Bryson, 2017; Giarla et al., 2014; Kajtoch et al., 2017; Kotsakiozi et al., 2018; Sheridan and Stuart, 2018; Shirley et al., 2014).

The Shangcheng stout salamander (*Pachyhynobius shangchengensis*) (Hynobiidae, Caudata) is a stream salamander, narrowly distributed in high elevation areas in the Dabie Mountains in Eastern China, at the junction of Henan, Hunan and Anhui provinces (Fei et al., 2012). It is endemic to the cool and oxygen-rich mountain streams above 500 meters in elevation. Previously, the subadult of *P. shangchengensis* had been recognized as *Hynobius yunanicus* due to the different morphological characters (e.g. white spots on the back and smaller body size) (Nishikawa et al., 2010; Xiong et al., 2007). Currently, *P. shangchengensis* had been classified as Vulnerable (B1ab) by the IUCN (http://www.iucnredlist.org/details/59109/0) because of population decline resulting mainly from over-collection for human consumption and habitat loss driven by farming activities and human settlements (Fei et al., 2012). Previous phylogeographic studies of *P. shangchengensis* revealed strong evidence that deep genetic divergences existed among different lineages and that the divergence between clades occurred over one million years ago (Pan et al., 2014; Pan et al., 2019; Zhao et al., 2013). These findings strongly suggest that *Pachyhynobius* may represent a multispecies complex. Consequently, a comprehensive assessment of the species number contextualized with evolutionary history is necessary to disclose the species conservation status, which will contribute to the development of an effective

management plan.

Here, we sequenced the complete mitochondrial genomes of individuals from six regional populations across the entire range of *P. shangchengensis*, and used them to generate phylogenetic reconstructions of the mitochondrial gene tree. Beyond resolving the phylogenetic relationships in *Pachyhynobius*, the availability of complete mitochondrial genomes can provide sufficient information to reconstruct the evolution and timescale of changes in this genus. In addition, a series of species-delimitation methods were used to clarify species boundaries and to identify candidate species within the genus, *Pachyhynobius*.

2. Materials and methods

2.1. Ethics Statements

In this study, the sample collection was performed by a long-term investigation project on amphibians of Dabie Mountains. This investigation project and the sample collection were approved by Anhui Tianma National Nature Reserve, Anhui Province, China. The relevant document of field permit is provided in the supplementary material.

2.2. Sampling

Samples of 35 individuals were collected from 16 locations during 2012-2015 in six isolated geographic areas representing the distribution range of *P. shangchengensis*: Jiaoyuan-Tanghui-Xiaolongtan (JTX, 7 individuals),

Kangwangzhai- Huangbaishan-Jiufengjian (KHJ, 6 individuals), Mazongling-Wochuan (MW, 6 individuals), Tiantangzhai (TTZ, 8 individuals), Baimajian-Yaoluoping-Mingtangshan (BYM, 7 individuals) and Kujingyuan (KJY, 1 individual; Fig. 1). We captured *P. shangchengensis* adults using dip nets and cut the tip of the tail (about 1 cm) prior to releasing them. All samples were preserved in 100% ethanol in the wild and then stored at -80°C until use. Total DNA was extracted from samples using a standard proteinase K/phenol-chloroform protocol (Sambrook et al., 1989). The DNA extraction used EasyPure Purification Kit (TransGene Biotech, Beijing, China) to purify.

2.3. PCR amplification

The complete mitochondrial genomes were amplified with PCR using mitochondrial primers designed with Primer Premier version 5.0 based on the mitochondrial genomes of *P. shangchengensis* (NC008080) and *Ranodon sibiricus* (NC004021) (Table S1) (Clarke and Gorley, 2001). PCR reaction mixtures (25 μL) for each gene consisted of 1 μL total DNA (concentration 10-50 ng/μL), 2.5 μL 10× buffer, 1 μL of 2.5 mM $MgSO_4$, 2 μL of 2 mM dNTPs, 1 U *Taq* polymerase (TransGene Biotech, Beijing, China), 0.3 mM of each primer and sufficient pure molecular biology grade water. The amplification protocol consisted of the following steps: an initial denaturation step of 95°C for 5 min, 32 cycles of denaturation at 95°C for 30 s, primer annealing at 53°C for 30 s and an extension at 72°C for 90 s, and a final extension at 72°C for 10 min. All PCR products were purified with a EasyPure

174 Purification Kit, and sequenced on an ABI Prism 3730 automated sequencer using the
175 BigDye Terminator v3.0 Ready Reaction Cycle Sequencing Kit (Applied
176 Biosystems).
177
178 **2.4. Sequence data preparation**
179 Sequences were assembled with Seqman II (DNAStar, Madison, WI, USA) and
180 visually inspected to ensure the accuracy of variable sites (Burland, 2000). BLAST
181 search and translation test methods were employed to exclude the potential nuclear
182 mitochondrial pseudogenes (Yao et al., 2008). Sequences were aligned using Clustal
183 X version 2.0 (Larkin et al., 2007). The known complete mtDNA sequences of *P.*
184 *shangchengensis* (NC008080) were used to identify protein-coding genes, and the 22
185 tRNA genes were identified by tRNA Scan-SE version 1.21
186 (http://lowelab.ucsc.edu/tRNAscan-SE 1.2.1). All assembled and annotated
187 mitochondrial genomes were submitted to GenBank (MK890366-MK890400, Table
188 S2).
189 The complete mitochondrial genomes generated in this study and those of
190 Hynobiidae publicly available in NCBI were used to reconstruct the phylogenetic tree
191 between taxa without partitions using Bayesian methods and Maximum Likelihood
192 (ML), with *Andrias davidianus* and *A. japonicus* as outgroups (Fig. 2). All
193 alignment-ambiguous regions were removed to avoid erroneous phylogenetic
194 hypotheses, and alignment gaps were analyzed as missing data.
195

196 **2.5. Mitochondrial phylogeny**

197 The best-fit DNA sequence evolution model of our dataset was estimated with
198 jModeltest.0.1 using the Bayesian Information Criterion (BIC) to choose the most
199 suitable model (Darriba et al., 2012). The Bayesian phylogenetic tree was inferred
200 using MrBayes version 3.1.2 (http://mrbayes.csit.fsu.edu/index.php) (Huelsenbeck
201 and Ronquist, 2001) and the best-fit model identified with jModeltest. Two
202 independent runs of MrBayes' Markov Chain Monte Carlo (MCMC) algorithm were
203 performed to assess convergence of posterior probability distributions. The run
204 parameters used were set 1×10^7 iterations of the MCMC algorithm sampled every
205 1,000 iterations, and discarding the first 10% of the iterations as burn-in. An average
206 standard deviation of split frequencies of 0.01 was used for checking model stability.

207 RaxML version 8 (Stamatakis, 2014) was used to perform ML analyses with a
208 general time reversible model of nucleotide substitution under the Gamma model of
209 rate heterogeneity (i.e., GTRCAT), with 1000 bootstrap iterations to determine
210 internal branch support of the best-scoring tree.

211

212 **2.6. Divergence-Time Analyses**

213 To estimate divergence times between different clades in *Pachyhynobius*, we
214 used BEAST version 1.8.0 (Drummond et al., 2012) to calculate an ultrametric tree
215 using as calibration points information (a, 157.1 Ma, 95% Highest Posterior Density
216 [HPD] = 145.6 – 165.3 Ma; b, 135.1 Ma, 95% HPD = 120.2 – 150.3 Ma; c, 40.2 Ma,
217 95% HPD = 34.5 – 46.2 Ma; Fig. 2) from a previous phylogenetic study of

Hynobiidae (Chen et al., 2015). For this analysis, we used a relaxed uncorrelated log normal model of lineage variation, a Yule Process prior for the branching rates, and with a GTR + I + G model of sequence evolution (best selected model). Four replicates of the analysis were run for 1×10^7 generations with parameter and tree sampling every 1,000 generations, discarding the first 25% of BEAST's MCMC iterations as burn-in. Convergence between runs was monitored using Tracer version 1.6 (Rambaut et al., 2014) and ESS values indicative of adequate sampling (i.e. >200). The phylogenetic tree was generated and visualized with TreeAnnotator version 1.8.0 (Rambaut and Drummond, 2010) and FigTree version 1.4.3 (Rambaut, 2016), respectively. The ultrametric tree without outgroups used for species delimitation was collected from this generated tree.

2.7. Species delimitation

We used SPLITSTREE version 4.13.1 (Huson and Bryant, 2006) to construct a phylogenetic network based on uncorrected p-distances with heterozygous ambiguities averaged and normalized, using the neighbor-net ordinary least squares variance and equal angle algorithm and 1,000 bootstrap replicates to assess branch support. We used several species delimitation models to determine the number of different species in our dataset. We used the BF approach (Grummer et al., 2013) to estimate the best fitting model to our dataset between alternative models (M1: 5 species; M2: 4 species; M3: 3 species; M4: 1 species) defined by the estimates of population structure identified by the above phylogenetic tree. The MLE of each

240 model was estimated and the BF between pairs of modes was calculated as BF = 2 ×
241 (MLE model1 – MLE model2)], with values for BF between 0 and 1 indicating very
242 weak support for model 1 over 2, values between 1 and 3 indicating some support,
243 albeit little, for model 1, values between 3 and 5 indicating strong support for model 1,
244 and values > 5 indicating decisive support for model 1 (Kass and Raftery, 1995). .
245 Two independent runs for each model were performed in *BEAST (Heled and
246 Drummond, 2010) to assess convergence of the MCMC runs. *BEAST was run each
247 time for 1 $\times 10^7$ generations of the MCMC algorithm sampling every 1,000
248 generations and discarding the first 25% of the iterations as "burn-in". The general
249 parameter settings were a relaxed uncorrelated log normal model of lineage variation,
250 a Yule Process prior for the branching rates, and with a GTR + I + G model of
251 sequence evolution. For MLE analysis, the applied parameters were as follows: 1×10^6
252 generations, sampling every 1,000 generations and default settings for the other
253 parameters. The results of different runs were combined using LogCombiner. Based
254 on the MLE results, the species tree of *Pachyhynobius* was determined. Convergence
255 of all model parameters was assessed by examining the trace plots and histograms in
256 Tracer.

257 BPP version 3.0 was used to simulate the posterior probabilities of speciation
258 events resulting in fewer or more lineages than the observed data using a reversible
259 jump MCMC (rjMCMC) algorithm (Rannala and Yang, 2003; Yang and Rannala,
260 2010). A guide tree to start the BPP analyses was generated from the species tree
261 estimated with MrBayes. The root age (τ) and prior distributions of the ancestral

262 population size (θ) can affect the posterior probabilities for the BPP models. Due to
263 the lack of knowledge about these parameters in *Pachyhynobius*, we tested the effect
264 of different prior values for τ and θ on the probabilities of posterior speciation. Three
265 ranges for θ were used, i.e. large G(1, 10), middle ~G(1, 100) and small ~G(2, 2000)
266 ancestral population size, and three ranges for τ representing divergences ranging
267 from deep to shallow genealogies, i.e. ~ G(1, 10), τ ~ G(1, 100) and τ ~ G (2, 2000).
268 BPP's run parameters were set to 500,000 generations sampling every 50 steps and
269 discarding the first 100,000 iterations as burn-in. Each BPP analysis of different
270 combinations of θ and τ priors was run twice to test algorithm convergence.

271 In addition to the Bayesian methods tested, we also applied three tree-based
272 species-delimitation methods, namely the single-threshold General Mixed Yule
273 Coalescent (sGMYC) (Pons et al., 2006; Tomochika and Barraclough, 2013), the
274 multiple threshold GMYC (mGMYC) (Monaghan et al., 2009) and Bayesian
275 implementation of the Poisson Tree Processes (bPTP) (Zhang et al., 2013). All three
276 analyses were calculated using the online server (http://species.h-its.org/). BEAST's
277 ultrametric tree with an outgroup (*R. sibiricus*) was used for the sGMYC, mGMYC
278 and bPTP models with default parameter settings in the server. The parameters of
279 these three analyses were set as follows: 500,000 generations, a thinning of 500 and
280 burn-in of 10%. Convergence of model was assessed by visualizing plots of MCMC
281 iteration vs. log likelihood. Lastly, we used the computationally efficient
282 distance-based species-delimitation method ABGD (Kekkonen and Hebert, 2014;
283 Puillandre et al., 2012a; Puillandre et al., 2012b), which can quantify the barcode gap

location that separates intra- from interspecific distances. During the calculation, default settings were used for the prior range for maximum intraspecific divergence (0.001, 0.1) and minimum slope increase (X) of 1.5 (default) and 1.0. Both JC69 and K80 corrected distances were used to compare species delimitation results.

3. Results

3.1. Sequences variability and trees construction

The aligned mtDNA genome from Hynobiidae and outgroups consisted of 16,575 bp nucleotide positions before trimming, and 16,553 bp after trimming. The trimmed data were used for genealogical reconstructions, including 8,105 constant and 8,378 variable sites. This dataset yielded well-supported phylogenetic trees (BI and ML; Fig. 2) with both reflecting the same topological structure previously identified for Hynobiidae (Chen et al., 2015; Zhang et al., 2006). All *Pachyhynobius* individuals formed a clade that internally presented five well supported groups (posterior probabilities = 1 and bootstrap support values = 100%), each representing a geographical area, namely JTX, KHJ, MW, TTZ and the two sampling areas that could not be genetically told apart, BYM and KJY (Fig. 2). These five lineages grouped forming two branches, one containing the JTX and KHJ lineages, and the other one the remaining 3 groups. The phylogenetic network of *Pachyhynobius* contained the same groupings observed with the phylogenetic methods (Fig. 3).

The dating analyses of Hynobiidae suggested that the most recent common ancestor (MRCA) of *Pachyhynobius* dates to ~7.84 million years ago (Ma; 95% HPD

306 = 5.62 – 13.09 Ma; Fig. 2). The MRCA of JTX and KHJ was ~3.19 Ma (95%HPD =
307 1.93 – 5.47 Ma). The MRCA of BYM, MW and TTZ was estimated at ~5.92 Ma (95%
308 HPD = 4.03 – 8.40 Ma), while the MRCA of MW and TTZ was ~3.25 Ma (95% HPD
309 = 2.15 – 5.33 Ma).
310
311 **3.2. Species delimitation**
312 The Bayes Factor for the comparison between the five candidate species
313 hypotheses and either the PS or SS hypotheses was larger than five, indicating that the
314 5-species hypothesis was clearly better than the other two alternatives (Table 1). The
315 BPP analysis supported the BF analysis, with all nine combinations of the values of
316 the priors for τ and θ presenting a posterior probability of at least 0.99 for the
317 hypothesis of 5 species (Table 2). The ABGD analysis suggested a total of five
318 species based on initial partitioning over a range of prior values for the maximum
319 intraspecific divergence observed (Fig. S1). However, as the divergence was reduced,
320 the number of inferred species decreased to three with a maximum intraspecific
321 divergence prior value (P) of 0.0055, or less if a lower threshold was allowed. The
322 sGMYC model yielded 6 clusters and 7 entities. In contrast, the mGMYC model (i.e.
323 several coalescent time values) shows 5 GMYC clusters and 7 entities (Fig. S2). bPTP
324 also suggested a strikingly high number of *Pachyhynobius* species (5) with confidence
325 intervals (4-7) from MCMC analyses (Fig. S3). Overall, the species tree (Fig. 4) was
326 highly consistent with the mtDNA gene tree.
327 Four out of six of the species-delimitation methods consistently identified five

328 species, while the sGMYC and mGMYC identified more than five. The areas of KHJ
329 and MW consistently presented one species per area. However, for both the sGMYC
330 and mGMYC methods the TTZ area presented two candidate species, while the BYM
331 area also presented two species with the sGMYC method, and the JTX area presented
332 two species with the mGMYC method (Table 3). Average pairwise sequence
333 divergence varied markedly among candidate species, from 1.8 % (JTX vs KHJ) to
334 4.1% (KHJ vs MW) (Table 4).
335
336 **4. Discussion**
337 **4.1. Species delimitation of *Pachyhynobius***
338 Generally, one of the main criteria for species delimitation is reciprocal
339 monophyly (Kizirian and Donnelly, 2004). In species delimitation, analytical methods
340 of delimiting species that typically rely upon the genetic distances across lineages or
341 the topological structure of a phylogenetic tree (Sites and Marshall, 2003, 2004)
342 require subjective setting of the thresholds that demarcate the species boundary (Hey,
343 2009). However, for recent speciation events, not all molecular markers are presumed
344 to be reciprocally monophyletic across the phylogenetic tree (Fujita and Al, 2012;
345 Hudson and Coyne, 2002). Recently, it has been possible to identify derived species
346 before achieving reciprocal monophyly after species formation (Knowles and
347 Carstens, 2007). In such cases where there is incomplete lineage sorting,
348 coalescent-based species delimitation approaches can be calculated that do not require
349 reciprocal monophyly of molecular markers or fixed differences (Fujita and Al, 2012;

Leaché and Fujita, 2010). In recent years, these methods for species delimitation have been successfully applied to many animal groups, such as sap-green stream frog (Ranidae: *Sylvirana*) (Sheridan and Stuart, 2018), horned lizards (Phrynosomatidae: *Phrynosoma*) (Blair and Bryson, 2017), Kotschy's gecko (Gekkonidae, *Mediodactylus*) (Kotsakiozi et al., 2018), Slender-snouted crocodilian (*Mecistops cataphractus*)(Shirley et al., 2014), and Andean mouse opossums (Didelphidae: *Thylamys*)(Giarla et al., 2014). These many examples demonstrate that these methods are successful in delimiting species boundaries for species complexes or morphologically indistinguishable species.

In this study we found that the inferred phylogenetic tree for the Chinese salamander *Pachyhynobius* using whole mitochondrial DNA sequences was consistent with previous phylogeographic analyses using single or multiple mitochondrial genes (Pan et al., 2014; Pan et al., 2019; Zhao et al., 2013), confirming the existence of five independent genetic clades within the genus. We found that two areas (KHJ and MW) consistently presented support for the existence of putative species in each of them across the various species-delimitation methods used (Table 3). In the species-tree approach (Fig. 4), the statistical support for the three additional lineages of JTX, TTZ, and BYM-KJY was very high (>90%). The signal supporting the identification of a candidate species for each geographic area in the *Pachyhynobius* distribution range was overall strong, as reflected by most species-delimitation methods supporting the presence of five candidate species. However, two of the methods suggested that a further number of hidden species may

372 remain. mGMYC suggested two potential candidate species within the JTX and TTZ
373 lineages, while sGMYC suggested two potential species within the TTZ and BYM
374 lineages. Although it is possible that these two GMYC based methods may be more
375 sensitive to otherwise subtle cryptic divergence in the data, it is also possible that they
376 may be too liberal when defining the number of putative species in a group as has
377 previously been suggested (Blair and Bryson, 2017; Lang et al., 2015). Contrastingly,
378 ABGD based on JC69 and K80 corrected distances indicated that there were fewer
379 species (3 instead of 5), defined as "JTX-KHJ", "MW-TTZ", and "BYM-KJY", or
380 less if lower maximum divergence thresholds were used. These results are
381 conservative in comparison to the GMYC models, and likely representative of the
382 reliance of the ABGD approach just on genetic distances without considering the
383 phylogenetic relationships between the operational taxonomic units studied (Postaire
384 et al., 2016). The genetic distance values among the five lineages were variable,
385 ranging from 1.8% to 4.1%. Overall, the genetic distances were close to intra-genus
386 genetic distances observed in Hynobiidae. For example, in the genus *Hynobius*, the
387 inter-species genetic distances ranged from 1.1% (*H. formosanus* vs *H. arisanensis*) to
388 11.2% (*H. formosanus* vs *H. kimurae*). Therefore, in this study, the species
389 delimitation based on mitochondrial genome data revealed that there are indeed
390 multiple species in *Pachyhynobius*. Of six species-delimitation methods used, four
391 methods strongly supported that there are five determined species (from JTX, KHJ,
392 MW, TTZ, BYM-KJY respectively).
393

4.2. Sky island effect and montane speciation

Abiotic factors such as climate and tectonic events, as well as biological factors such as interspecific or intraspecific interactions, competition and predation, may be the major drivers for biological evolution and diversification temporally and geographically (Benton, 2009). Generally, due to the interactions of multiple abiotic and biological factors, mountains exhibit various microhabitats with different ecological conditions than the surrounding landscape. Herein, unique and endemic species often evolved with the relatively small populations that are separated by well-defined geographical boundaries (Huang et al., 2017; Shepard and Burbrink, 2009, 2011). In the vast subtropical regions of China, countless scattered mountains (e.g., Qinling Mountains, Hengduan Mountains, Dabie Mountains) form potential sky islands, which show spatial isolation on restricted areas and are considered ideal natural laboratories for studying the formation of endemic plants and animal species (Gao et al., 2015; Zhen et al., 2016).

After the rapid uplift, the Tibetan Plateau and its adjacent mountain ranges acted as a blocky orographic barrier to the atmospheric circulation, and then contributed to the Asian monsoon system (Guo et al., 2008; Song et al., 2010; Tang et al., 2013). During three East Asian monsoon intensification periods (~15 Ma, ~8 Ma and 4-3 Ma) (Jacques et al., 2011; Molnar et al., 2010; Wan et al., 2007), the monsoonal flow led to the humid and warm climate in the south of China (Sun and Wang, 2005). This was favorable for speciation and geographical spreading (Che et al., 2010; Wu et al., 2013). Mountainous areas often harbor more cryptic lineages because altitudinal

zonation of habitats and rugged terrain cause the formation of sky island habitats (He and Jiang, 2014; McCormack et al., 2009). For these species restricted to sky-island habitats, dispersal often was limited and more opportunities were created for allopatric divergence, which promotes high levels of inter-population genetic divergence and unique patterns of genetic structure (Favre et al., 2015; Kozak and Wiens, 2006; Pauls et al., 2006; Shepard and Burbrink, 2008, 2009, 2011; Valbuenaureña et al., 2017; Wu et al., 2013; Zhu et al., 2011). For example, in western Arkansas (USA), unique physiographic features of the Ouachita Mountains area, coupled with species response to climatic factors, drove deep lineage divergence in three *Plethodon* species (*P. ouachitae*, *P. fourchensis* and *P. caddoensis*) and finally produced a series of classic phylogeographic structures associated with stream drainages and mountains (Shepard and Burbrink, 2008, 2009, 2011).

Pachyhynobius is a typical stream salamander, endemic to the Dabie Mountains, and lives in the cool and oxygen-rich streams above 500 meters in elevation (Fei et al., 2012)**.** In this study, dating analyses of Hynobiidae suggested that the MRCA of *Pachyhynobius* dates back to ~7.84 Ma (Fig. 2), while the five candidate species originated ~3.19 to ~5.92 Ma (Fig. 2). The deep genetic divergences were disclosed among these candidate species (Fig. 2, 3 and 4), which indicated that the candidate species may be separated long-term by unsuitable habitats. Dabie Mountains, composed of a chain of ancient isolated low-middle elevation massifs (Fig. 1), were believed to be able to maintain a relatively stable climate over the last several million years (Ju et al., 2007; Zhao et al., 2009). In addition, ecology niche model (ENM)

indicated that lower elevation areas acted as a strict and effective isolation barrier for the *Pachyhynobius* species (Pan et al., 2019). Therefore, once discontinuous sky islands were formed and fixed, deep inter-species genetic divergences of *Pachyhynobius* gradually accumulated, then monophyletic groups appeared, and finally, the independent species formed.

5. Conclusion

In this study, different species delimitation approaches revealed that multiple species exist in the genus *Pachyhynobius*. Although these methods failed to produce an identical species number, most species delimitation methods indicated that there are five distinct species (from JTX, KHJ, MW, TTZ, BYM-KJY respectively) in *Pachyhynobius*. Discontinuous habitat, combined with niche conservatism, produced the sky-island effect in *Pachyhynobius* and finally led to hidden species diversity in this genus.

Author contributions

BWZ led the research team. BWZ, XBW and TP designed the research. TP, ZLS, HW, PY and BWZ collected samples. TP, ZLS and WQZ performed research. TP, XLL, SZL, PY, HW and GYW analyzed data. TP, HW and PO wrote the paper.

Funding

This work was supported by the National Natural Science Foundation of China

(Grant No. 31272332), National Key Research and Development Program (2016YFC1200705), Anhui Province Higher Education Revitalization Plan, 2014 Colleges and Universities Outstanding Youth Talent Support Program, 2017 Anhui Province academic and technical leaders candidates (2017H130), Anhui Natural Science Foundation (Youth, 1908085QC127), Research start-up funds of Anhui Normal University (751865).

Acknowledgements

We thank Mr. Zhaojie Peng, Mr. Lifu Qian, Miss Yanan Zhang, Miss Xin Kang for their help in sample collecting and data analysis. We thank Dr. Jackson R. Richards for his linguistic assistance. We thank Associate Editor (Allan Larson) and two anonymous reviewers for their suggestions.

REFERENCES

Agapow, P.-M., Bininda-Emonds, O.R.P., Crandall, K.A., Gittleman, J.L., Mace, G.M., Marshall, J.C., Purvis, A., 2004. The impact of species concept on biodiversity studies. Q. Rev. Biol. 79, 161–179.

Aldhebiani, A.Y., 2018. Species concept and speciation. Saudi. J. Biol. Sci. 25, 437–440.

Benton, M.J., 2009. The Red Queen and the Court Jester: species diversity and the role of biotic and abiotic factors through time. Science 323, 728–732.

Bickford, D., Lohman, D.J., Sodhi, N.S., Ng, P.K.L., Meier, R., Winker, K., Ingram, K.K., Das, I., 2007. Cryptic species as a window on diversity and conservation. Trends Ecol. Evol. 22, 148–155.

Blair, C., Bryson, J.R., 2017. Cryptic diversity and discordance in single-locus species delimitation methods within horned lizards (Phrynosomatidae: *Phrynosoma*). Mol. Ecol. Res. 17, 1–15.

Burland, T.G., 2000. DNASTAR's Lasergene sequence analysis software. Methods Mol. Biol. 132, 71–91.

Catarina, R., David James, H., Salvador, C., Luís, M., Ana, P., 2016. The taxonomy of the *Tarentola mauritanica* species complex (Gekkota: Phyllodactylidae): Bayesian species delimitation supports six candidate species. Mol. Phylogenet. Evol. 94, 271–278.

Che, J., Zhou, W.W., Hu, J.S., Yan, F., Papenfuss, T.J., Wake, D.B., Zhang, Y.P., 2010. Spiny frogs (*Paini*) illuminate the history of the Himalayan region and Southeast Asia. P. Natl. Acad. Sci. 107, 13765–13770.

Chen, M.Y., Mao, R.L., Liang, D., Kuro-O, M., Zeng, X.M., Zhang, P., 2015. A reinvestigation of phylogeny and divergence times of Hynobiidae (Amphibia, Caudata) based on 29 nuclear genes. Mol. Phylogenet. Evol. 83, 1–6.

Clarke, K.R., Gorley, R.N., 2001. Primer v5. Primer–E Ltd.

Darriba, D., Taboada, G.L., Doallo, R., Posada, D., 2012. JModelTest 2: more models, new heuristics and parallel computing. Nat. Methods 9, 772.

Dowle, E.J., Morgan-Richards, M., Brescia, F., Trewick, S.A., 2015. Correlation between shell phenotype and local environment suggests a role for natural selection in the evolution of *Placostylus* snails. Mol. Ecol. 24, 4205–4221.

Drummond, A.J., Suchard, M.A., Xie, D., Rambaut, A., 2012. Bayesian phylogenetics with BEAUti and the BEAST 1.7. Mol. Biol. Evol. 29, 1969–1973.

Fan, Y., Wu, R., Chen, M.H., Kuo, L., Lewis, P.O., 2011. Choosing among partition models in Bayesian phylogenetics. Mol. Biol. Evol. 28, 523–532.

Favre, A., Päckert, M., Pauls, S.U., Jähnig, S.C., Uhl, D., Michalak, I., Muellner‐Riehl, A.N., 2015. The role of the uplift of the Qinghai‐Tibetan Plateau for the evolution of Tibetan biotas. Biol. Rev. 90, 236–253.

Fei, L., Ye, C.Y., Jiang, J.P., 2012. Colored Atlas of Chinese Amphibians and their Distributions. Sichuan Publishing House of Science and Technology, Chengdu.

Fujisawa, T., Barraclough, T.G., 2013. Delimiting species using single-locus data and the generalized mixed Yule coalescent approach: a revised method and evaluation on simulated data sets. Syst. Biol. 62, 707–724.

Fujita, M.K., Al, E., 2012. Coalescent-based species delimitation in an integrative taxonomy. Trends Ecol. Evol. 27, 480–488.

Gao, Y., Ai, B., Kong, H.H., Kang, M., Huang, H.W., 2015. Geographical pattern of isolation and diversification in karst habitat islands: a case study in the *Primulina eburnea* complex. J. Biogeogr. 42, 2131–2144.

Giarla, T.C., Voss, R.S., Jansa, S.A., 2014. Hidden diversity in the Andes: comparison of species delimitation methods in montane marsupials. Mol. Phylogenet. Evol. 70, 137–151.
Grummer, J.A., Jr, B.R., Reeder, T.W., 2013. Species delimitation using Bayes factors: simulations and application to the *Sceloporus scalaris* species group (Squamata: Phrynosomatidae). Syst. Biol. 63, 119–133.
Guo, Z.T., Sun, B., Zhang, Z.S., Peng, S.Z., Xiao, G.Q., Ge, J.Y., Hao, Q.Z., Qiao, Y.S., Liang, M.Y., Liu, J.F., 2008. A major reorganization of Asian climate by the early Miocene. Clim. Past 4, 153–174.
Hausdorf, B., 2011. Progress toward a general species concept. Evolution 65, 923–931.
He, K., Jiang, X.L., 2014. Sky islands of southwest China. I: an overview of phylogeographic patterns. Chinese Sci. Bull. 59, 585 – 597.
Heled, J., Drummond, A.J., 2010. Bayesian inference of species trees from multilocus data. Mol. Biol. Evol. 27, 570–580.
Hey, J., 2009. On the arbitrary identification of real species. Cambridge University Press, Cambridge, UK.
Huang, Z.S., Yu, F.L., Gong, H.S., Song, Y.L., Zeng, Z.G., Zhang, Q., 2017. Phylogeographical structure and demographic expansion in the endemic alpine stream salamander (Hynobiidae: *Batrachuperus*) of the Qinling Mountains. Sci. Rep. 7, 1–13.
Hudson, R.R., Coyne, J.A., 2002. Mathematical consequences of the genealogical species concept. Evolution 56, 1557–1565.
Huelsenbeck, J.P., Ronquist, F., 2001. MrBayes: Bayesian inference of phylogenetic trees. Bioinformatics 17, 754–755.
Huson, D.H., Bryant, D., 2006. Application of phylogenetic networks in evolutionary studies. Mol. Biol. Evol. 23, 254–267.
Jacques, F.M.B., Guo, S.X., Su, T., Xing, Y.W., Huang, Y.J., Liu, Y.S., Ferguson, D.K., Zhou, Z.K., 2011. Quantitative reconstruction of the Late Miocene monsoon climates of southwest China: a case study of the Lincang flora from Yunnan Province. Palaeogeogr. Palaeocl. 304, 318–327.
Ju, L., Wang, H., Jiang, D., 2007. Simulation of the Last Glacial Maximum climate over East Asia with a regional climate model nested in a general circulation model. Palaeogeogr. Palaeocl. 248, 376–390.
Kajtoch, Ł., Montagna, M., Wanat, M., 2017. Species delimitation within the *Bothryorrhynchapion* weevils: Multiple evidence from genetics, morphology and ecological associations. Mol. Phylogenet. Evol. 120, 354–363.
Kass, R.E., Raftery, A.E., 1995. Bayes factors. J. Am. Stat. Assoc. 90, 773–795.
Kekkonen, M., Hebert, P.D., 2014. DNA barcode-based delineation of putative species: efficient start for taxonomic workflows. Mol. Ecol. Res. 14, 706–715.
Kizirian, D., Donnelly, M.A., 2004. The criterion of reciprocal monophyly and classification of nested diversity at the species level. Mol. Phylogenet. Evol. 32, 1072–1076.
Knowles, L.L., Carstens, B.C., 2007. Delimiting species without monophyletic gene trees. Syst. Biol. 56, 887–895.
Kotsakiozi, P., Jablonski, D., Ilgaz, Ç., Kumlutaş, Y., Avcı, A., Meiri, S., Itescu, Y., Kukushkin, O., Gvoždík, V., Scillitani, G., 2018. Multilocus phylogeny and coalescent species delimitation in Kotschy's gecko, *Mediodactylus kotschyi*: hidden diversity and cryptic species. Mol. Phylogenet. Evol. 125, 177–187.
Kozak, K.H., Wiens, J.J., 2006. Does niche conservatism promote speciation? A case study in North American salamanders. Evolution 60, 2604–2621.
Lande, R., 1976. Natural selection and random genetic drift in phenotypic evolution. Evolution 30,

559 314–334.
560 Lang, A.S., Bocksberger, G., Stech, M., 2015. Phylogeny and species delimitations in European
561 *Dicranum* (Dicranaceae, Bryophyta) inferred from nuclear and plastid DNA Mol. Phylogenet. Evol. 92,
562 217–225.
563 Larkin, M.A., Blackshields, G., Brown, N.P., Chenna, R., McGettigan, P.A., McWilliam, H., Valentin, F.,
564 Wallace, I.M., Wilm, A., Lopez, R., Thompson, J.D., Gibson, T.J., Higgins, D.G., 2007. Clustal W and
565 Clustal X version 2.0. Bioinformatics 23, 2947–2948.
566 Leaché, A.D., Fujita, M.K., 2010. Bayesian species delimitation in West African forest geckos
567 (*Hemidactylus fasciatus*). P. Roy. Soc. Lond. B Biol. 277, 3071–3077.
568 Li, W.L.S., Drummond, A.J., 2012. Model averaging and Bayes factor calculation of relaxed molecular
569 clocks in Bayesian phylogenetics. Mol. Biol. Evol. 29, 751–761.
570 McCormack, J.E., Huang, H., Knowles, L.L., Gillespie, R., Clague, D., 2009. Sky islands. Encyclopedia of
571 Islands 4, 841–843.
572 Molnar, P., Boos, W.R., Battisti, D.S., 2010. Orographic controls on climate and paleoclimate of Asia:
573 thermal and mechanical roles for the Tibetan Plateau. Annu. Rev. Earth Pl. Sc. 38, 77–102.
574 Monaghan, M.T., Wild, R., Elliot, M., Fujisawa, T., Balke, M., Inward, D.J.G., Lees, D.C., Ranaivosolo, R.,
575 Eggleton, P., Barraclough, T.G., 2009. Accelerated species inventory on Madagascar using
576 coalescent-based models of species delineation. Syst. Biol. 58, 298–311.
577 Nevo, E., 2001. Evolution of genome-phenome diversity under environmental stress. Proc. Natl. Acad.
578 Sci. 98, 6233–6240.
579 Nishikawa, K., Jiang, J.P., Matsui, M., Mo, Y.M., Chen, X.H., Kim, J.B., Tominaga, A., Yoshikawa, N., 2010.
580 Invalidity of *Hynobius yunanicus* and molecular phylogeny of *Hynobius* salamander from continental
581 China (Urodela, Hynobiidae). Zootaxa 2426, 65–67.
582 Pan, T., Wang, H., Hu, C.C., Shi, W.B., Zhao, K., Huang, X., Zhang, B.W., 2014. Range–wide
583 phylogeography and conservation genetics of a narrowly endemic stream salamander, *Pachyhynobius*
584 *shangchengensis* (Caudata, Hynobiidae): implications for conservation. Genet. Mol. Res. 13, 2873–
585 2885.
586 Pan, T., Wang, H., Pablo, O., Hu, C.C., Wu, G.Y., Qian, L.F., Sun, Z.L., Shi, W.B., Yan, P., Wu, X.B., Zhang,
587 B.W., 2019. Long-term sky islands generate highly divergent lineages of a narrowly distributed stream
588 salamander (*Pachyhynobius shangchengensis*) in mid-latitude mountains of East Asia. BMC Evol. Biol.
589 (Accepted).
590 Pauls, S.U., Lumbsch, T., Haase, P., 2006. Phylogeography of the montane caddisfly *Drusus discolor*:
591 evidence for multiple refugia and periglacial survival. Mol. Ecol. 15, 2153–2169.
592 Pons, J., Barraclough, T.G., Gomez-Zurita, J., Cardoso, A., Duran, D.P., Hazell, S., Kamoun, S., Sumlin,
593 W.D., Vogler, A.P., 2006. Sequence-based species delimitation for the DNA taxonomy of undescribed
594 insects. Syst. Biol. 55, 595–609.
595 Postaire, B., Magalon, H., Bourmaud, A.F., Bruggemann, J.H., 2016. Molecular species delimitation
596 methods and population genetics data reveal extensive lineage diversity and cryptic species in
597 Aglaopheniidae (Hydrozoa). Mol. Phylogenet. Evol. 105, 36–49.
598 Puillandre, N., Lambert, A., Brouillet, S., Achaz, G., 2012a. ABGD, Automatic Barcode Gap Discovery for
599 primary species delimitation. Mol. Ecol. 21, 1864–1877.
600 Puillandre, N., Modica, M.V., Zhang, Y., Sirovich, L., Boisselier, M.C., Cruaud, C., Holford, M., Samadi, S.,
601 2012b. Large-scale species delimitation method for hyperdiverse groups. Mol. Ecol. 21, 2671–2691.
602 Rambaut, A., 2016. FigTree v1.4.3; 2016. Available at: http://tree.bio.ed.ac.uk/software/figtree/.

Rambaut, A., Drummond, A.J., 2010. TreeAnnotator version 1.8; 2016. Available at: http://beast.community/programs.

Rambaut, A., Suchard, M., Xie, D., Drummond, A.J., 2014. MCMC Trace Analysis Package (version 1.6); 2014. Available at: http://tree.bio.ed.ac.uk/software/tracer/.

Rannala, B., Yang, Z.H., 2003. Bayes estimation of species divergence times and ancestral population sizes using DNA sequences from multiple loci. Genetics 164, 1645-1656.

Sambrook, J., Fritsch, E.F., Maniatis, T., 1989. Molecular cloning. Cold Spring Harbor Laboratory Press, New York.

Shepard, D.B., Burbrink, F.T., 2008. Lineage diversification and historical demography of a sky island salamander, *Plethodon ouachitae*, from the Interior Highlands. Mol. Ecol. 17, 5315 – 5335.

Shepard, D.B., Burbrink, F.T., 2009. Phylogeographic and demographic effects of Pleistocene climatic fluctuations in a montane salamander, *Plethodon fourchensis*. Mol. Ecol. 18, 2243–2262.

Shepard, D.B., Burbrink, F.T., 2011. Local-scale environmental variation generates highly divergent lineages associated with stream drainages in a terrestrial salamander, *Plethodon caddoensis*. Mol. Phylogenet. Evol. 59, 399–411.

Sheridan, J.A., Stuart, B.L., 2018. Hidden species diversity in *Sylvirana nigrovittata* (Amphibia: Ranidae) highlights the importance of taxonomic revisions in biodiversity conservation. PLoS One 13, e0192766.

Shirley, M.H., Vliet, K.A., Carr, A.N., Austin, J.D., 2014. Rigorous approaches to species delimitation have significant implications for African crocodilian systematics and conservation. Proc. Biol. Sci. 281, 20132483.

Sites, J.W., Marshall, J.C., 2003. Delimiting species: a renaissance issue in systematic biology. Trends Ecol. Evol. 18, 462–470.

Sites, J.W., Marshall, J.C., 2004. Operational criteria for delimiting species. Ann. Rev. Ecol. Evol. Syst. 35, 199–227.

Song, J.H., Kang, H.S., Byun, Y.H., Hong, S.Y., 2010. Effects of the Tibetan Plateau on the Asian summer monsoon: a numerical case study using a regional climate model. Int. J. Climatol. 30, 743–759.

Stamatakis, A., 2014. RaxML version 8: a tool for phylogenetic analysis and post-analysis of large phylogenies. Bioinformatics 30, 1312–1313.

Sun, X.G., Wang, P.X., 2005. How old is the Asian monsoon system?—Palaeobotanical records from China. Palaeogeogra. Palaeocl. 222, 181–222.

Svanback, R., Eklov, P., 2006. Genetic variation and phenotypic plasticity: causes of morphological and dietary variation in Eurasian perch. Evol. Ecol. Res. 8, 37–49.

Tang, H., Micheels, A., Eronen, J.T., Ahrens, B., Fortelius, M., 2013. Asynchronous responses of East Asian and Indian summer monsoons to mountain uplift shown by regional climate modelling experiments. Clim. Dynam. 40, 1531–1549.

Tomochika, F., Barraclough, T.G., 2013. Delimiting species using single-locus data and the generalized mixed Yule coalescent approach: a revised method and evaluation on simulated data sets. Syst. Biol. 62, 707–724.

Valbuenaureña, E., Solermembrives, A., Steinfartz, S., Orozcoterwengel, P., Carranza, S., 2017. No signs of inbreeding despite long-term isolation and habitat fragmentation in the critically endangered Montseny brook newt (*Calotriton arnoldi*). Heredity 118, 1–12.

Wagner, C.E., Keller, I., Wittwer, S., Selz, O.M., Mwaiko, S., Greuter, L., Sivasundar, A., Seehausen, O., 2013. Genome-wide RAD sequence data provide unprecedented resolution of species boundaries and relationships in the Lake Victoria cichlid adaptive radiation. Mol. Ecol. 22, 787–798.

Wan, S.M., Li, A.C., Clift, P.D., Stuut, J.B.W., 2007. Development of the East Asian monsoon: mineralogical and sedimentologic records in the northern South China Sea since 20 Ma. Palaeogeogra. Palaeocl. 254, 561–582.

Wu, Y.K., Wang, Y.Z., Jiang, K., Hanken, J., 2013. Significance of pre-Quaternary climate change for montane species diversity: insights from Asian salamanders (Salamandridae: *Pachytriton*). Mol. Phylogenet. Evol. 66, 380–390.

Xie, W.G., Lewis, P.O., Fan, Y., Kuo, L., Chen, M.H., 2011. Improving marginal likelihood estimation for Bayesian phylogenetic model selection. Syst. Biol. 60, 150–160.

Xiong, J.L., Chen, Q., Zeng, X.M., Zhao, E.M., Qing, L.Y., 2007. Karyotypic, Morphological, and Molecular Evidence for *Hynobius yunanicus* as a Synonym of *Pachyhynobius shangchengensis* (Urodela: Hynobiidae). J. Herpetol. 41, 664–671.

Yang, Z.H., Rannala, B., 2010. Bayesian species delimitation using multilocus sequence data. P. Natl. Acad. Sci. USA 107, 9264–9269.

Yao, Y.G., Kong, Q.P., Salas, A., Bandelt, H.J., 2008. Pseudomitochondrial genome haunts disease studies. J. Med. Genet. 45, 769–772.

Zhang, J., Kapli, P., Pavlidis, P., Stamatakis, A., 2013. A general species delimitation method with applications to phylogenetic placements. Bioinformatics 29, 2869–2876.

Zhang, P., Chen, Y.Q., Zhou, H., Liu, Y.F., Wang, X.L., Papenfuss, T.J., Wake, D.B., Qu, L.H., 2006. Phylogeny, evolution, and biogeography of Asiatic salamanders (Hynobiidae). P. Natl. Acad. Sci. USA 103, 7360–7365.

Zhao, B., Zhang, J., Sun, X.H., 2009. Eco-environmental vulnerability evaluation based on GIS in Tongbai–Dabie Mountain area of Huai River Basin. Res. Soil Water Conserv. 16, 135–138.

Zhao, Y.Y., Zhang, Y.H., Li, X.C., 2013. Molecular phylogeography and population genetic structure of an endangered species *Pachyhynobius shangchengensis* (hynobiid Salamander) in a fragmented habitat of southeastern China. PLoS One 8, e78064.

Zhen, Y., Chen, P.P., Bu, W.J., 2016. Terrestrial mountain islands and Pleistocene climate fluctuations as motors for speciation: a case study on the genus *Pseudovelia* (Hemiptera: Veliidae). Sci. Rep. 6, 33625.

Zhu, L.F., Zhang, S.N., Gu, X.D., Wei, F.W., 2011. Significant genetic boundaries and spatial dynamics of giant pandas occupying fragmented habitat across southwest China. Mol. Ecol. 20, 1122–1132.

678 **Titles and legends to figures**

679 **Fig. 1:** Sampling area and regional group of *Pachyhynobius* in Dabie Mountains,
680 China. The dotted lines represent rivers. The values with different colors
681 represent the elevations of mountains. Sampling sites are shown as ellipses. The
682 approximate position of the region within China is shown in the inset as a green
683 square.

684

685 **Fig. 2:** Mitochondrial genomic phylogeny of the Hynobiidae. The species from
686 *Pachyhynobius* are shown with a pink background. The values on nodes indicate
687 Bayesian posterior probabilities and ML bootstrap support (shown as a
688 percentage). These letters (a, b and c) indicate the calibration points. The blue
689 lines on nodes correspond to the 95% highest posterior density of the age of the
690 node. The bottom axis is in millions of years.

691

692 **Fig. 3:** Network constructed from the complete mitochondrial genome of the
693 *Pachyhynobius* samples based on uncorrected p-distances using SPLITSTREE.
694 The values on nodes indicate bootstrap support (only values above 75% are
695 shown).

696

697 **Fig. 4:** Species tree estimated using BEAST based on complete mitochondrial
698 genome in *Pachyhynobius*. The values on nodes are Bayesian posterior
699 probabilities.

Fig. S1: Species delimitation analyses by ABGD methods with two model (JC90 and K80l) based on complete mitochondrial genome in *Pachyhynobius*. Y-axis shows the number of groups inferred, and the x-axis the maximum divergence threshold used for species delimitation. The two models show identical results of species delimitation.

Fig. S2: Lineage through time plots in the species delimitation analyses by sGMYC method (A) and mGMYC method (B) based on complete mitochondrial genomes in *Pachyhynobius*. N represents the lineage number. Vertical red line(s) indicate the inflection point between speciation and coalescence. Branching events older than the inferred threshold indicating speciation event, while younger ones representing coalescences within species. The bottom axis is in millions of years.

Fig. S3: Species delimitation analyses by bPTP methods based on complete mitochondrial genomes in *Pachyhynobius*. The putative molecular species identified are marked beside the tree. The numbers above branches correspond to the nodes' support posterior probabilities.

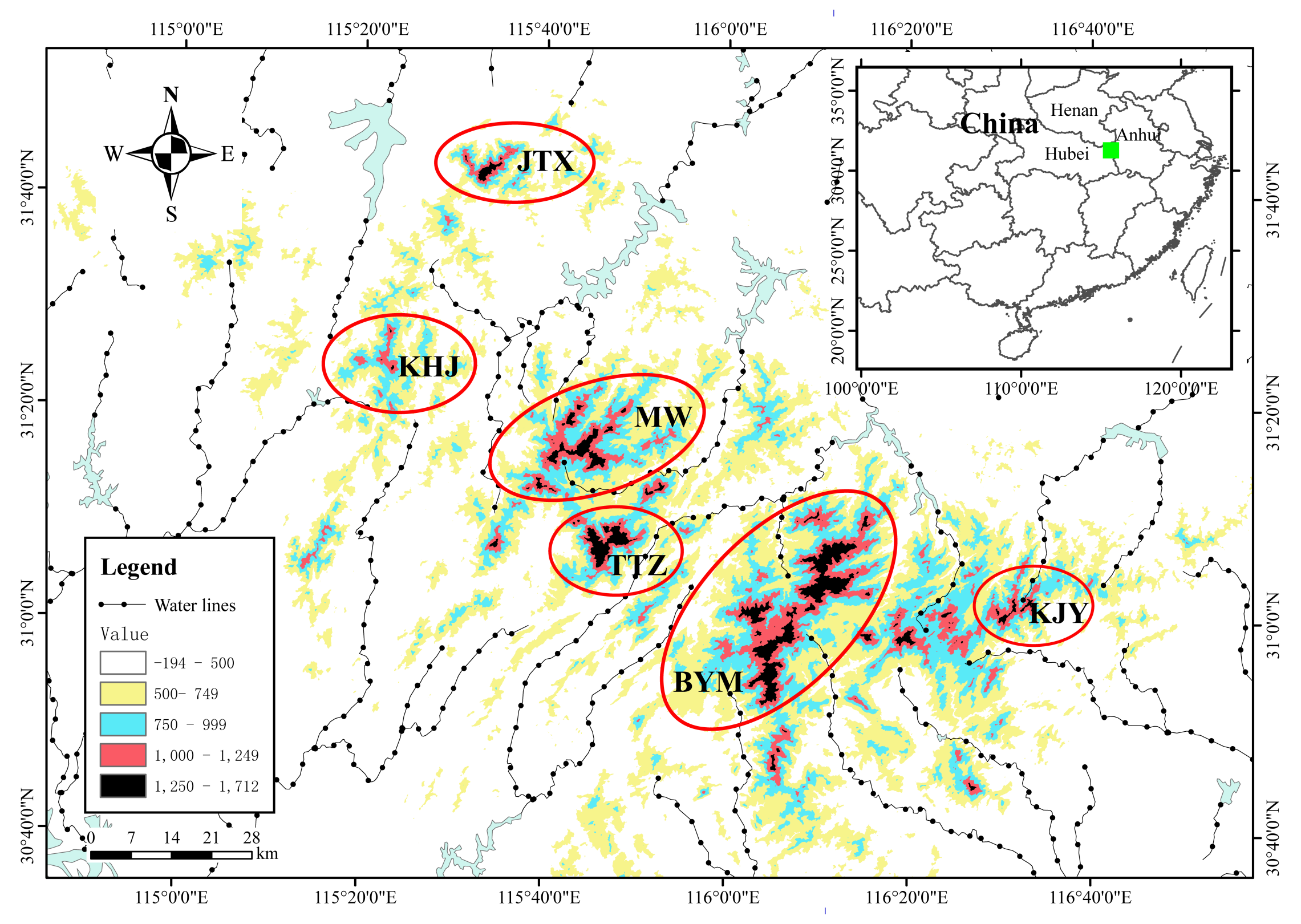
115°0'0"E
115°20'0"E
115°40'0"E
116°0'0"E
116°20'0"E
116°40'0"E
31°40'0"N
31°20'0"N
31°0'0"N
30°40'0"N
N
W
E
S
JTX
KHJ
MW
TTZ
BYM
KJY
China
Henan
Anhui
Hubei
100°0'0"E
110°0'0"E
120°0'0"E
35°0'0"N
30°0'0"N
25°0'0"N
20°0'0"N
Legend
Water lines
Value
-194 - 500
500- 749
750 - 999
1,000 - 1,249
1,250 - 1,712
0 7 14 21 28
km

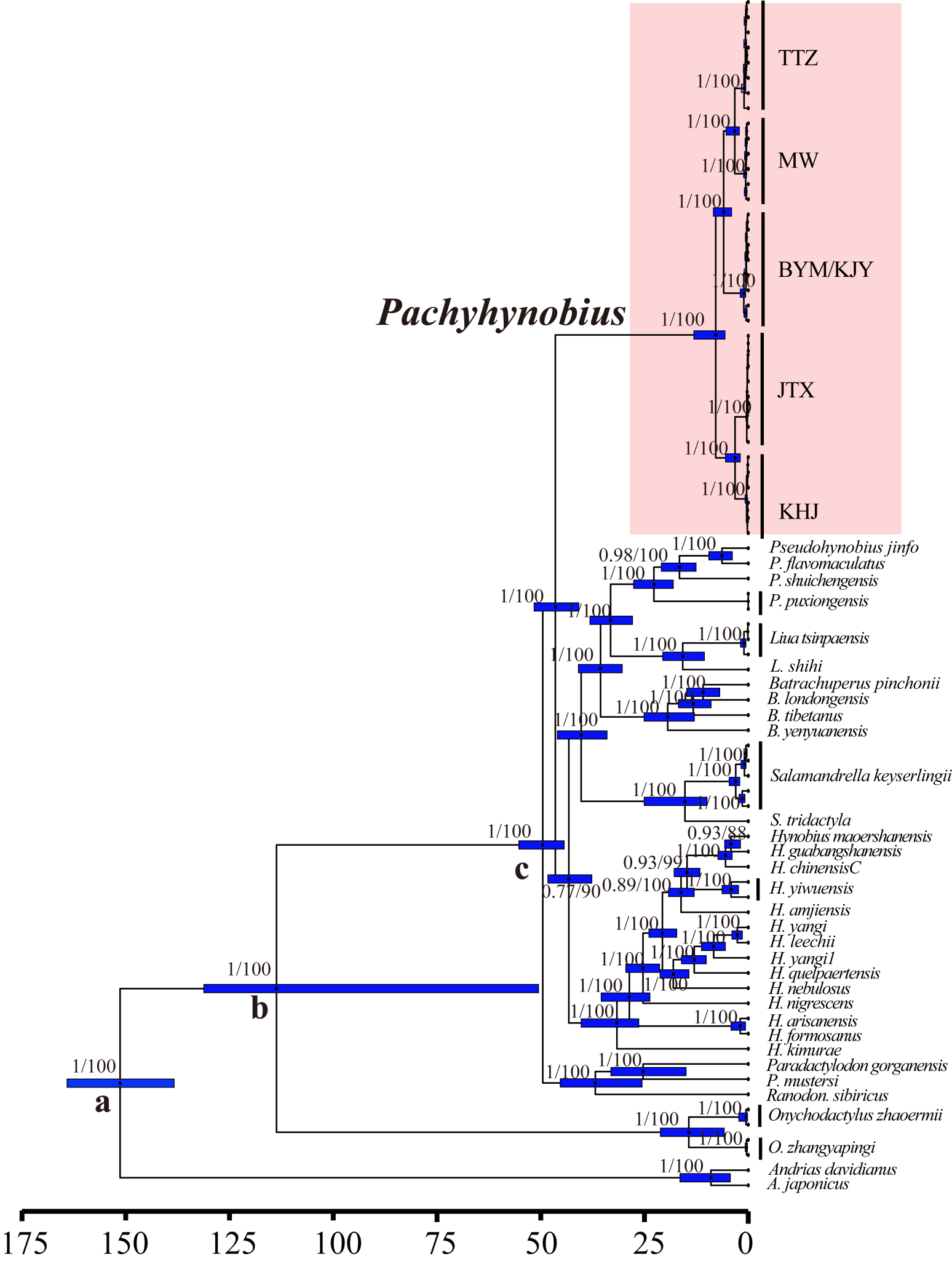
Pachyhynobius
TTZ
MW
BYM/KJY
JTX
KHJ
Pseudohynobius jinfo
P. flavomaculatus
P. shuichengensis
P. puxiongensis
Liua tsinpaensis
L. shihi
Batrachuperus pinchonii
B. londongensis
B. tibetanus
B. yenyuanensis
Salamandrella keyserlingii
S. tridactyla
Hynobius maoershanensis
H. guabangshanensis
H. chinensisC
H. yiwuensis
H. amjiensis
H. yangi
H. leechii
H. yangi1
H. quelpaertensis
H. nebulosus
H. nigrescens
H. arisanensis
H. formosanus
H. kimurae
Paradactylodon gorganensis
P. mustersi
Ranodon. sibiricus
Onychodactylus zhaoermii
O. zhangyapingi
Andrias davidianus
A. japonicus
a
b
c
175
150
125
100
75
50
25
0

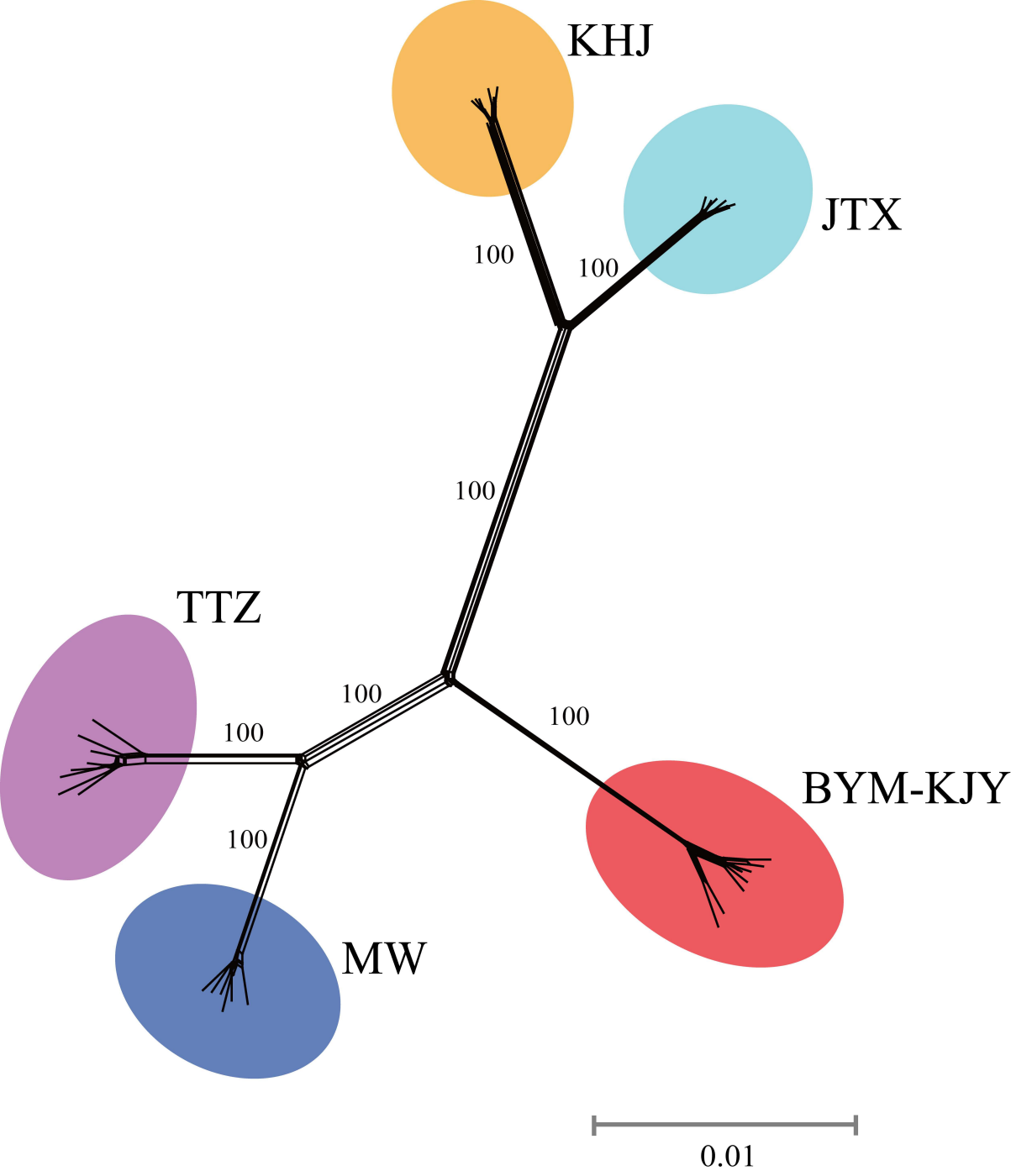
KHJ
JTX
TTZ
BYM-KJY
MW
100
100
100
100
100
100
0.01

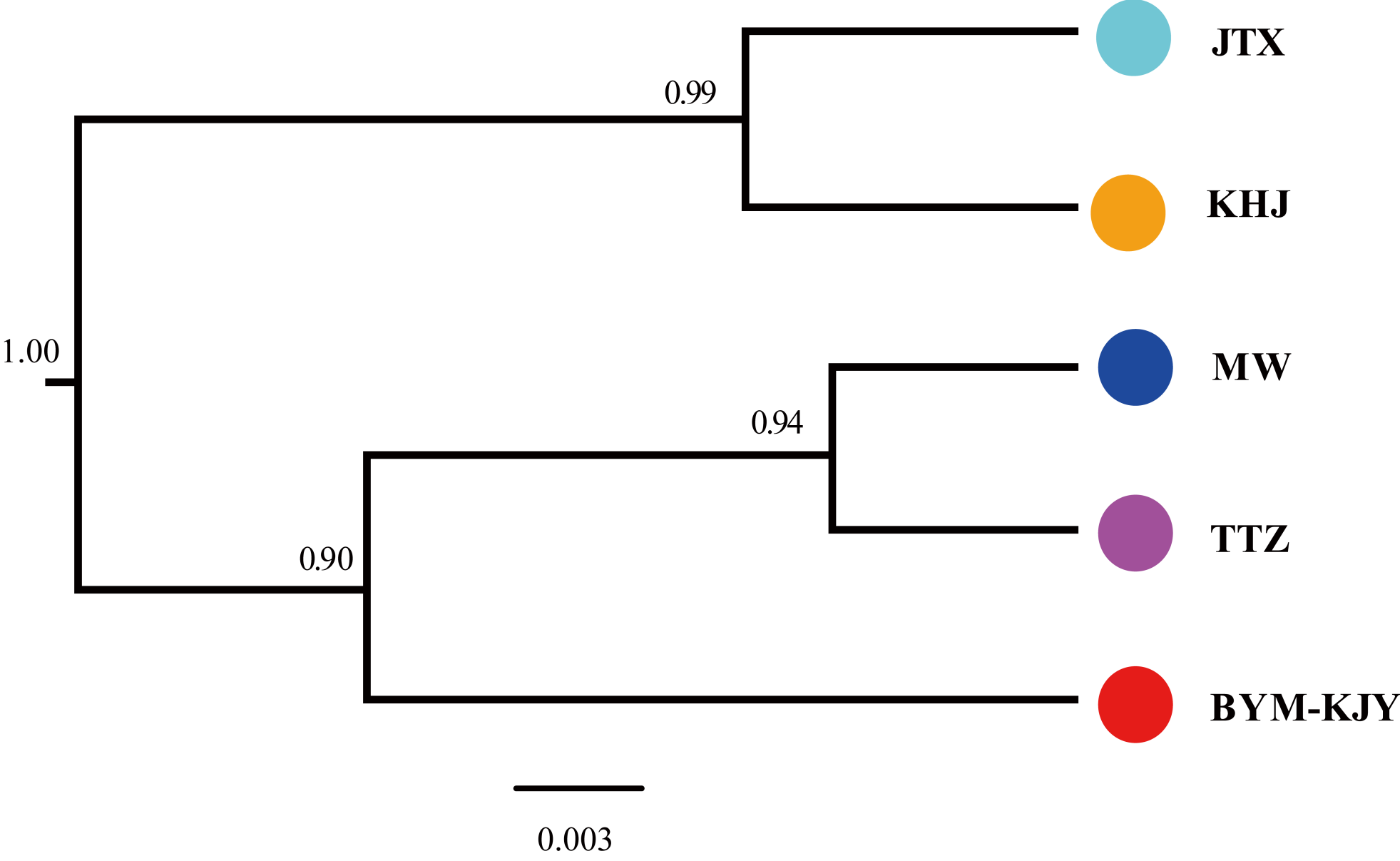
JTX
KHJ
MW
TTZ
BYM-KJY
0.99
1.00
0.94
0.90
0.003

Table 1. The Species Delimitation results of *Pachyhynobius* in BF method.

Model	Species	MLE Path Sampling(PS)	MLE Stepping Stone(SS)	Rank	BF	
					PS	SS
M1	5	–34243.11	–34243.18	1	16.08	16.06
M2	4	–34251.15	–34251.21	2	–	–
M3	3	–34256.11	–34256.19	3	–	–
M4 (current taxonomy)	1	–34292.29	–34292.44	4	–	–

Note: “MLE”represents “Marginal likelihood estimate”; “BF ”represents “Bayes factor”.

Table 2. The species delimitation results of *Pachyhynobius* in BPP method.

Scheme	Priordistribution		Posterior probabilities
	θ	τ	
Scheme 1	G (1,10)	G (1,10)	P[5]=0.9971
Scheme 2	G (1,10)	G (1,100)	P[5]=0.9948
Scheme 3	G (1,10)	G (1,2000)	P[5]=0.9908
Scheme 4	G (1,100)	G (1,10)	P[5]=0.9984
Scheme 5	G (1,100)	G (1,100)	P[5]=0.9988
Scheme 6	G (1,100)	G (1,2000)	P[5]=0.9987
Scheme 7	G (1,2000)	G (1,10)	P[3]=1.0000
Scheme 8	G (1,2000)	G (1,100)	P[3]=1.0000
Scheme 9	G (1,2000)	G (1,2000)	P[3]=0.9999

Note: “P[5]” represents“((KHJ, JTX), (BYM-KJY, (TTZ, MW)))”; “P[3]” represents“(BYM-KJY-MW-TTZ, (KHJ, JTX))”.

Table 3. Number of lineages in *Pachyhynobius* inferred by mutiple species delimitation methods.

Lineage	n	Mean Tamura–Nei distance	BF	GMYC single	GMYC multiple	bPTP	BPP	ABGD
JTX	8	0.001	1	1	2	1	1	1
KHJ	6	0.002	1	1	1	1	1	1
MW	6	0.003	1	1	1	1	1	1
TTZ	8	0.004	1	2	2	1	1	1
BYM-KJY	8	0.004	1	2	1	1	1	1
Total	36	0.0028	5	7 (5–14)	7 (5–7)	5.14(5–7)	5	5

Note: “n” represents the number of individuals; All bPTP are from Bayesian MCMC analyses. Confidence intervals for totals are in parentheses.

ABGD results are based on the initial partitioning scheme with a maximum intraspecific diversity value of 0.0055 (K80 distances).

Table 4. Pairwise F_{ST} among five candidate species (BYM-KJY, TTZ, MW, KHJ, JTX) of *Pachyhynobius*.

	BYM-KJY	TTZ	MW	KHJ	JTX
BYM-KJY					
TTZ	0.029*				
MW	0.031*	0.019*			
KHJ	0.039*	0.039*	0.041*		
JTX	0.037*	0.038*	0.039*	0.018*	

Note: Significant tests are indicated with an asterisk (*$P < 0.01$).

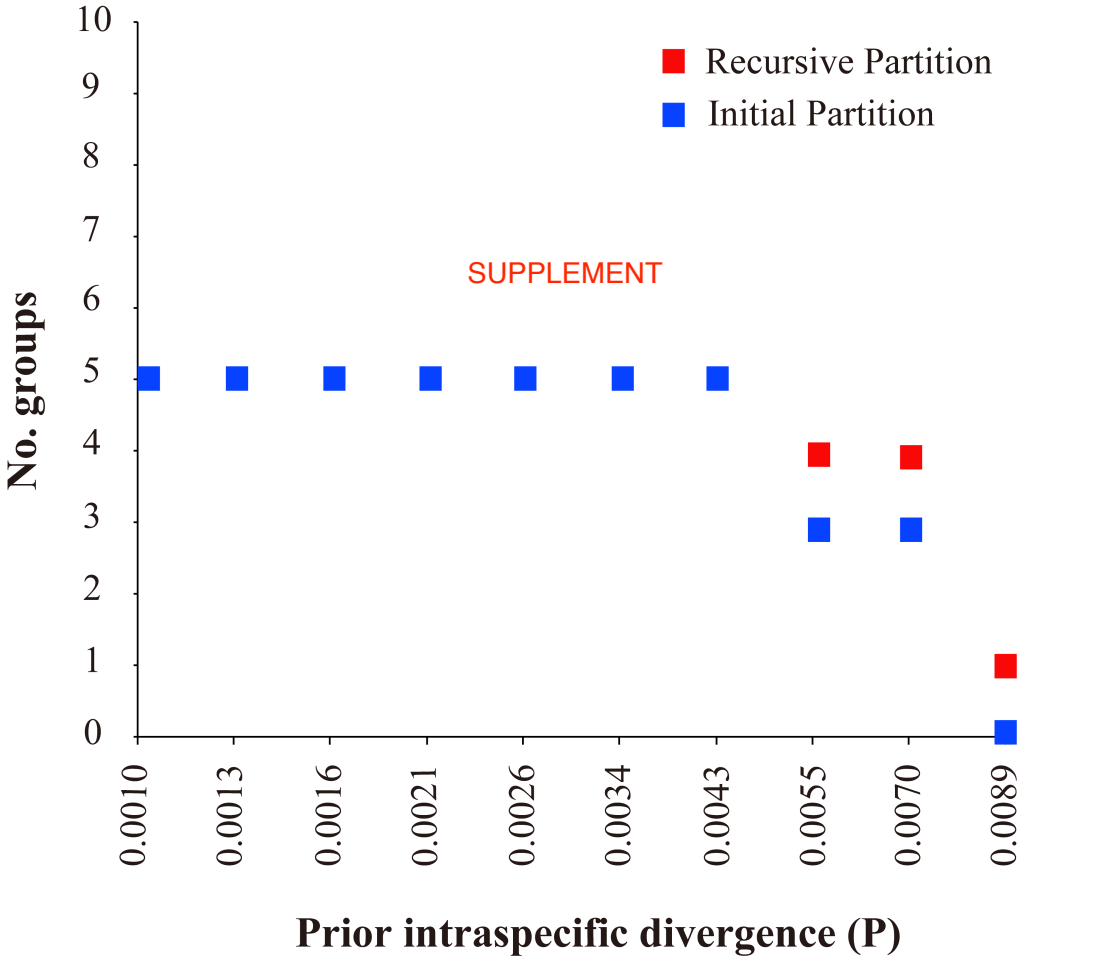
Recursive Partition
Initial Partition
SUPPLEMENT
No. groups
10
9
8
7
6
5
4
3
2
1
0
0.0010
0.0013
0.0016
0.0021
0.0026
0.0034
0.0043
0.0055
0.0070
0.0089
Prior intraspecific divergence (P)

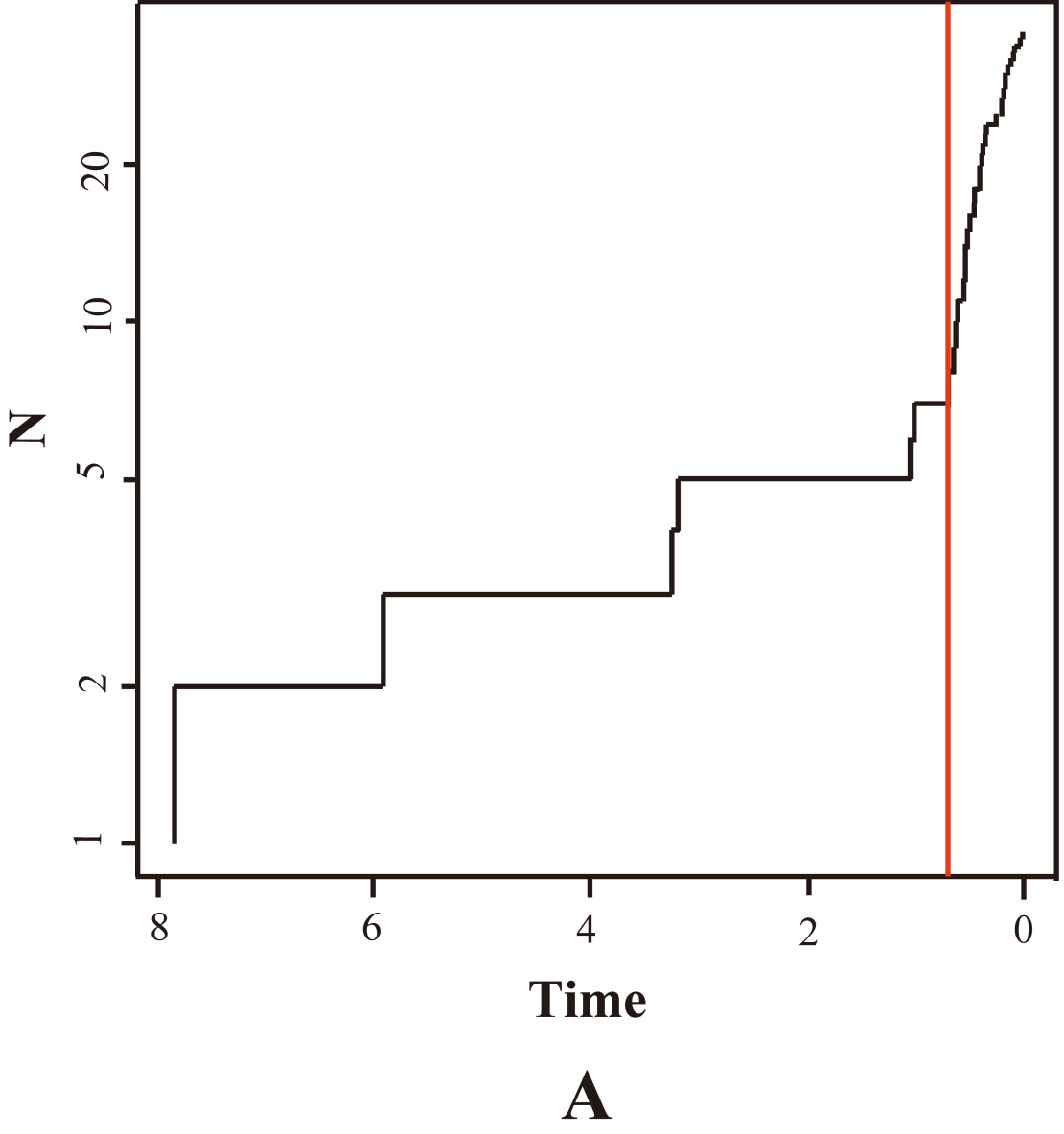

A

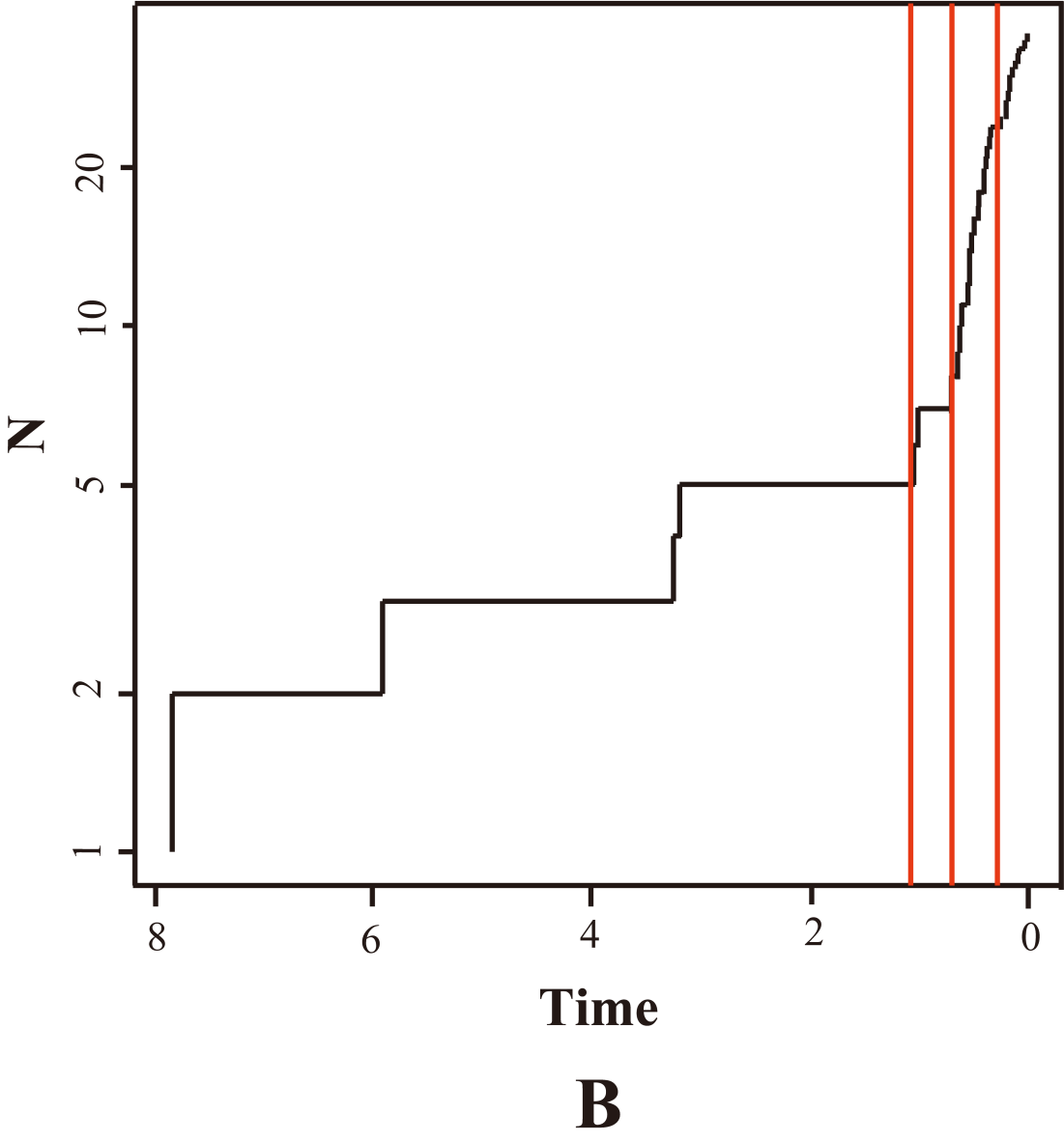

B

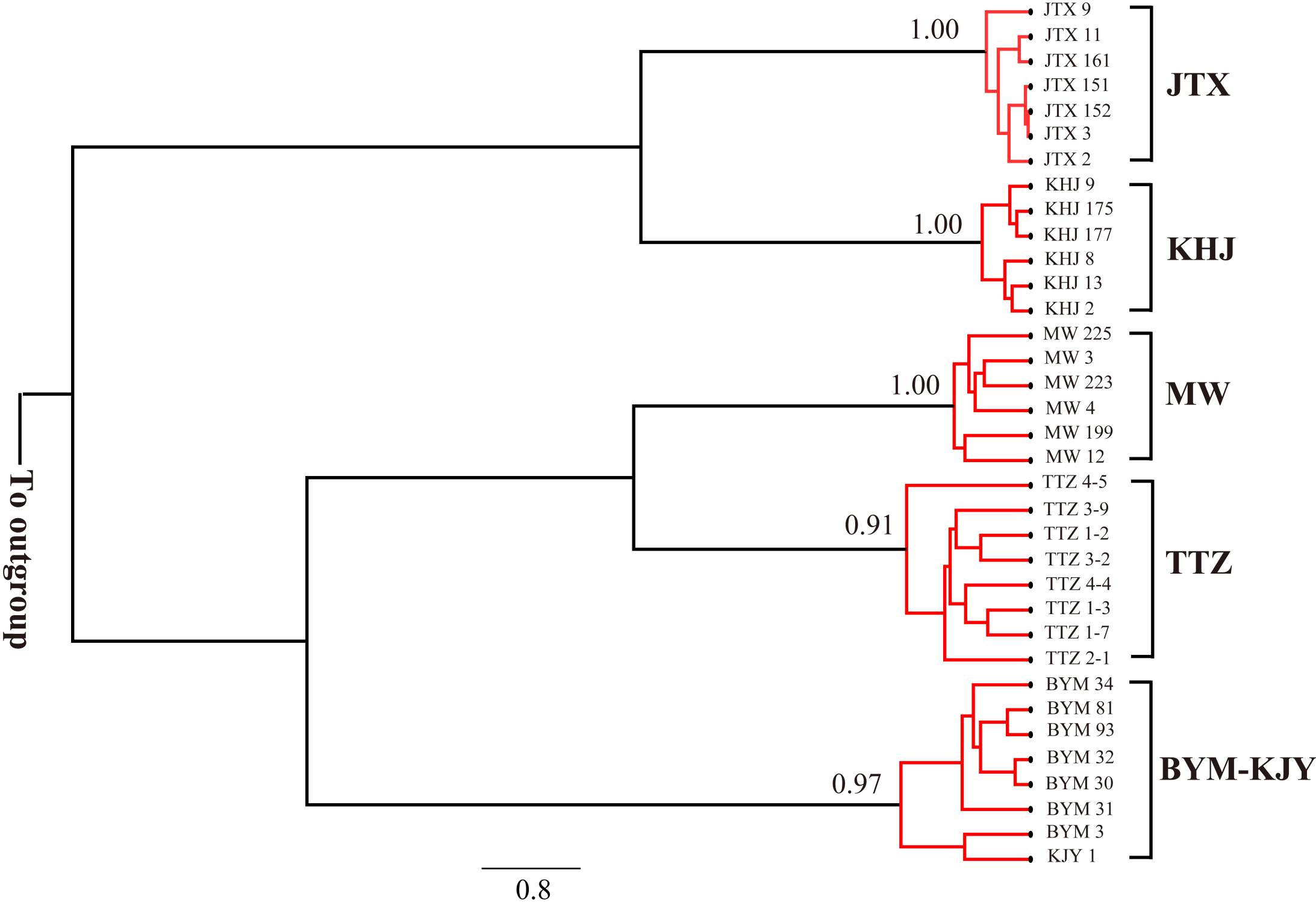
JTX 9
JTX 11
JTX 161
JTX 151
JTX 152
JTX 3
JTX 2
JTX
1.00
KHJ 9
KHJ 175
KHJ 177
KHJ 8
KHJ 13
KHJ 2
KHJ
1.00
MW 225
MW 3
MW 223
MW 4
MW 199
MW 12
MW
1.00
TTZ 4-5
TTZ 3-9
TTZ 1-2
TTZ 3-2
TTZ 4-4
TTZ 1-3
TTZ 1-7
TTZ 2-1
TTZ
0.91
BYM 34
BYM 81
BYM 93
BYM 32
BYM 30
BYM 31
BYM 3
KJY 1
BYM-KJY
0.97
To outgroup
0.8

Table S1. Primers for amplified the complete mitochondrial genome of *Pachyhynobius*.

Pairs	Primer name	Sequence (5' to 3')	Gene	Annealing temp. (℃)
1	Psh-1F26	GTTTATGTAGCTTAAACAAAGCATGG	12S	53
	Psh-1R1333	TCGGAGTAGCTCGTTTAGTTTC	16S	53
2	Psh-2F1054	GCTTACACCAAGAAGATACTCGT	16S	53
	Psh-2R2363	GCTGTTATCCCTAGGGTAACTT	16S	53
3	Psh-3F2333	CGAGAAGACCCTATGGAGC	16S	53
	Psh-3R3363	AAGCTCTGATTCCCCTTCAGTT	ND1	53
4	Psh-4F3116	GGCTCAGGATGATCATCAAATTC	ND1	53
	Psh-4R4326	CTATAGGTGCTAGTTTTTGTCAAGT	ND2	53
5	Psh-5F4065	AAACTTCATCACCCACGAGCAA	ND2	53
	Psh-5R5348	GTCATCGAGTGATTATCACAGGT	COX1	53
6	Psh-6F5067	CATCACCTGAATGCAACTCAGAT	COX1	53
	Psh-6R6348	CACAATATTGCGGCGTCTCATTT	COX1	53
7	Psh-7F6030	GACCCTGTACTTTACCAACATCT	COX1	53
	Psh-7R7478	ATACGAATTGGGGATTCTATTGGAA	COX2	53

8	Psh-8F7117	TCATGACCATGCATTAATAGCAGTTT	COX2	53
	Psh-8R8467	GCAATTAATTGAATTAATAAATGTCCGG	ATP6	53
9	Psh-9F8222	TCTAGGTTTATTACCATATACATTTACC	ATP6	53
	Psh-9R9359	CAACAAAATGTCAATATCATGCTGC	COX3	53
10	Psh-10F9106	GTAACCTGAGCTCATCATAGTATTAT	COX3	53
	Psh-10R10378	AATGGCGATGAAATAAAATCTACTCC	ND4	53
11	Psh-11F10137	AGGACTTGCATTAATAGTAGCTACT	ND4L	53
	Psh-11R11413	ATATACAATGTGTAGGAGGCTGTAAT	ND4	53
12	Psh-12F11181	CGCACTATTCTGCTTAGCAAATATAA	ND4	53
	Psh-12R12285	CTTGTATTGCTGCAGTATTTGCG	ND5	53
13	Psh-13F11928	GCATTTTTAATTAGCCTAACACCATTAA	ND5	53
	Psh-13R13168	CCTGAAACTATACTACCTCATGC	ND5	53
14	Psh-14F12941	GCACTCCATTTCTTGCTGGATTT	ND5	53
	Psh-14R14189	TTTTCGAATTGGGTGGGCCATTA	CYTB	53
15	Psh-15F13898	GCCAAAGAAGCAGAATACGCAAA	ND6	53
	Psh-15R15235	GATGCGGCTTGTCCAATTTCAAT	CYTB	53

16	Psh-16F14999	CTCATTACACCCCCACATATTCA	CYTB	53
	Psh-16R154	GGTCCTAGCCTTACTATTAATTGAAA	12S	53

Table S2 The complete mitochondrial genome of species in Hynobiidae with GeneBank accession nos. of corresponding sequences.

Taxonomy/Species name	Accession No.	Full Length(bp)
Order Caudata		
Family Hynobiidae		
Batrachuperus londongensis	NC008077	16,379
B. pinchonii	NC008083	16,390
B. tibetanus	NC008085	16,379
B. yenyuanensis	NC012430	16,394
Hynobius amjiensis	NC008076 (DQ333808)	16,401
H. arisanensis	NC009335 (EF462213)	16,401
H. chinensis	JQ710885	16,495
H. chinensis -CIB-XM2853	HM036353.1	16,404
H. formosanus	NC008084	16,394
H. guabangshanensis	NC013762	16,408
H. kimurae	JQ929920	16,448
H. leechii	NC008079 (DQ333811)	16,428
H. maoershanensis	NC023789	16,412
H. nebulosus	NC020650	16,447
H. nigrescens	NC026033	16,412
H. quelpaertensis	NC010224	16,407
H. yangi	NC013825	16,424
H. yangi-1	JN415127	16,403
H. yiwuensis	HM036354	16,494
Liua shihi	NC008078	16,376
L. tsinpaensis	NC008081	16,380
L. tsinpaensis –Tsinpa20141205	KP233806	16,378
Onychodactylus fischeri	NC008089	16,456
O. zhangyapingi	NC026853	16,537

O. zhangyapingi-1	KX021909	16,457
O. zhaoermii	KX021908	16,455
Pachyhynobius shangchengensis	NC008080	16,394
P. shangchengensis (JTX)	MK890394-MK890400	16,395-16,396
P. shangchengensis (KHJ)	MK890388-MK890393	16,393-16,394
P. shangchengensis (MW)	MK890382-MK890387	16,398-16,418
P. shangchengensis (TTZ)	MK890374-MK890381	16,397-16,400
P. shangchengensis (BYM)	MK890366-MK890370, MK890372, MK890373	16,396-16,399
P. shangchengensis (KJY)	MK890371	16,396
Protohynobius puxiongensis	FJ532058	16,398
Pseudohynobius jinfo	NC026698	16,393
P. flavomaculatus	NC020635	16,389
P. puxiongensis	NC020634	16,398
P. shuichengensis	NC021001	16,394
P. tsinpaensis	DQ333813	16,380
Paradactylodon mustersi	NC008090	16,383
P. gorganensis	NC008091	16,374
Ranodon sibiricus	NC004021	16,418
Salamandrella keyserlingii	DQ333814	16,338
S. keyserlingii -SK8321	JX508761	16,336
S. keyserlingii -SK8391	JX508762	16,340
S. keyserlingii -SK8440	JX508763	16,334
S. keyserlingii -SKN9	JX508764	16,338
S. tridactyla	NC021106	16,342
Order Caudata		
Family Cryptobranchidae		
Andrias davidianus	NC004926	16,503
A. japonicus	NC007446	16,298